Boundary Condition on Superfluid ^{3}He as Altered by ^{4}He Interfacial Layer

D. Kim, M. Nakagawa, O. Ishikawa, T. Hata, and T. Kodama
Faculty of Science, Osaka City University, Sumiyoshi-ku, Osaka 558, Japan

H. Kojima
Serin Physics Laboratory, Rutgers University, Piscataway, New Jersey 08854

(Received 14 June 1993)

The effects of the ^{4}He interfacial layer on the average superfluid fraction ($\hat{\rho}_s/\rho$) and the specularity (S) of quasiparticle scattering of superfluid ^{3}He were measured as a function of temperature, pressure, and pore size by means of fourth sound propagation. Up to a pore size dependent threshold ^{4}He coverage, both $\hat{\rho}_s/\rho$ and S remain equal to those for pure ^{3}He. Beyond the threshold, both rapidly increase as ^{4}He coverage is increased. The enhancements vanish at pressures greater than some critical pressures depending on ^{4}He thickness and pore size.

PACS numbers: 67.57.Np, 67.40.Hf, 67.40.Pm

The interaction of ^{3}He with its surrounding walls of the container, or perhaps heat exchanger, is important not only in understanding the properties of the ^{3}He liquid in such confined geometries but in refrigeration at low temperatures. As part of this general problem, the question of the boundary condition of superfluid ^{3}He at solid walls has attracted much theoretical and experimental attention. It is generally assumed that the specularity of ^{3}He quasiparticle scattering at the boundary walls determines the spatial dependence of the order parameter near the wall [1]. The physical relationship between the nature of the bounding wall and the specularity factor has not been established. Following the discovery by Freeman *et al.* [2] that the order parameter is enhanced by the ^{4}He interfacial layer, the ^{4}He coverage method has become an important tool for studying the boundary effects [3–6]. In this paper we report the first simultaneous measurements of the specularity factor and the concurrent enhancement of superfluid fraction of ^{3}He in a variety of pore structures and in the presence of ^{4}He coverage. The measurements were carried out as functions of ^{4}He thickness, pressure of ^{3}He, and the radius of pore space.

In our experiment, we use conventional fourth sound resonance techniques [7, 8] for measuring the superfluid fraction. The fourth sound is the pressure wave in the superfluid confined in small pores when the normal component is effectively immobilized by the viscous interaction with the wall of the pores. To the extent that the normal component moves relative to the stationary walls, the viscous stress leads to energy dissipation and to attenuation of fourth sound. In the low temperature range of this experiment where the mean free path becomes comparable to or greater than the pore radius, the ordinary hydrodynamic boundary condition ($v_n \rightarrow 0$ at the stationary wall) is modified to "slip" boundary condition. Jensen, Smith, and Wölfle [9] showed that the slip effect is dominant in the fourth sound attenuation and that the quality factor Q of an ideal straight cylindrical fourth sound resonator of pore radius R is given by

$$1/Q = (\omega {\rho_n}^2/\hat{\rho}_s)\kappa\zeta R/8\eta, \tag{1}$$

where ω is the resonance angular frequency. The slip length ζ may be approximated by (Maxwellian lower bound) [9], $\zeta = (4/3)[\eta/Np_F f^0(\Delta)](1+S)/(1-S)$, where η is the shear viscosity, p_F the Fermi momentum, N the particle number density, $f^0(\Delta)$ the Fermi-Dirac function at gap energy Δ, and S the specularity factor. We shall use Eq. (1) to extract the specularity from the measured quality factor.

In order to provide a direct comparison under the identical conditions of ^{4}He coverage, temperature, and pressure, we mounted four resonator cells simultaneously into a copper nuclear demagnetization apparatus. Each cylindrical cell (inner diameter of 8 mm, and length of 15 mm) was filled with a powder and closed at its ends with two capacitive transducers. Excellent thermal contact among the cells and to lanthanum-diluted CMN and Pt NMR thermometer is provided by 1 mm diam holes located at midpoint in each cell wall. The thickness of ^{4}He coverage is primarily determined by the surface area (220 m^2) of Pt-Ag powder heat exchanger and of course by the amount of ^{4}He introduced. The resonance frequency (< 9 kHz) and the quality factor (≤ 350) were determined from the frequency response of the receiver transducer to the driver transducer in the usual manner [7].

Alumina powders (taken from the same batch as those used by us previously) of nominal grain sizes 3, 1, and 0.3 μm are carefully packed to reproduce pore sizes of Ref. [10]. The silver powder (sintered for 1 h at 400 °C in helium atmosphere) is a nominally 700 Å powder [11]. The average pore radius of the silver packing is estimated from the magnitude of observed size effect.

The observed enhancement at a pressure of 5 bars in the superfluid fraction in a 3 μm cell is illustrated in Fig. 1. There is a substantial depression of the superfluid fraction from the bulk in pure ^{3}He. The magnitude of this size effect, its temperature, and pressure dependence are consistent in this and all of the other powders with our

0031-9007/93/71(10)/1581(4)$06.00

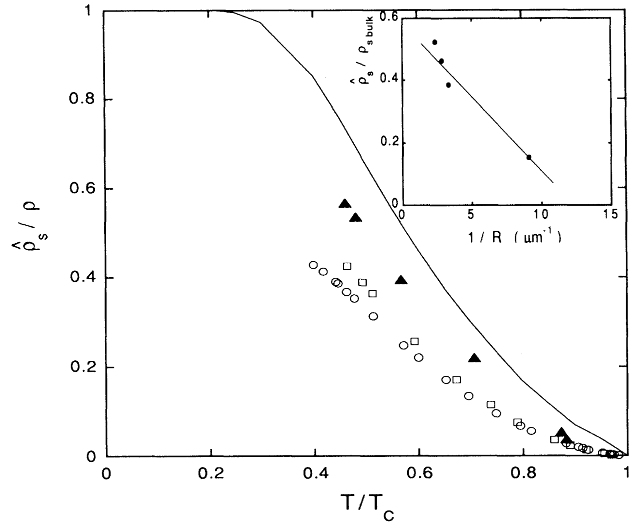

FIG. 1. Enhancement of superfluid fraction in 3 μm powder resonator at p= 5 bars. Open circles, pure ^{3}He and 1.1 layer ^{4}He coverage; squares, 1.9 layer coverage; triangles, 2.6 layer coverage. Solid line is the bulk superfluid fraction [J. Parpia *et al.*, J. Low Temp. Phys. **61**, 337 (1985)]. The inset shows the relative depression of the superfluid fraction of the pure ^{3}He as a function of the inverse pore radius.

earlier work [10]. In the inset to Fig. 1, the relative depression of the superfluid fraction in pure ^{3}He from the bulk value is plotted as a function of the inverse of the average pore radius. The critical radius at which the superfluid fraction becomes zero is very roughly estimated to be $2.3\xi_0$ ($\xi_0 = 350$ Å). Clearly more data are needed to establish the critical radius [12].

When 1.1 layers of ^{4}He are introduced [13] into the cells, the measured superfluid fraction overlaps that of the pure ^{3}He data at all pressures less than 27 bars. When 1.9 layers of ^{4}He are introduced, a small increase in the superfluid fraction becomes visible. Thereafter, the enhancement of the superfluid fraction is quite rapid. By 2.6 layer ^{4}He coverage, the superfluid fraction close to the bulk value is reached. Data with greater ^{4}He coverage (4.5 layers were attempted) could not be taken owing to extremely long thermal relaxation times.

How the superfluid fraction enhancement depends on the powder size as a function of the ^{4}He coverage is shown in Fig. 2. In pure ^{3}He, the depression of the superfluid fraction from the bulk value is greater as the powder size and the average pore radius are decreased as expected (see inset to Fig. 1). The threshold ^{4}He coverage at which superfluid enhancement begins to occur increases as the powder size decreases.

The effects of pressure are shown in Fig. 3 for the case of a 3 μm powder cell. The observed pressure dependence in the pure ^{3}He data arises from that of the coherence length. The results of ^{4}He coverage include data taken with both increasing and decreasing pressure. When 1.1

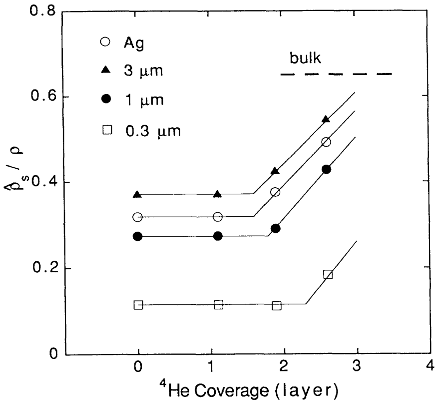

FIG. 2. ^{4}He coverage dependence of the superfluid fraction at $T/T_c = 0.47$ at $p = 5$ bars. The lines are guides for the eye.

layers of ^{4}He are deposited, the pressure dependence reproduces that of the pure ^{3}He at all pressures (these data are not shown). When ^{4}He coverage is increased to 1.9 layers the magnitude of the enhancement becomes sensitive to ^{3}He pressure. When the pressure is greater than 21($\pm$ 1) bars, the enhancement disappears and the pressure dependence again reproduces that of the pure ^{3}He data. When the ^{4}He coverage is increased to 2.6 layers, the pressure at which enhancement disappears increases to 24($\pm$ 1) bars. This coincides with the melting pressure of bulk ^{4}He. The pressure dependence in the lower pressure range (< 10 bars) arises from that of the bulk superfluid fraction not the coherence length.

Aside from the behavior near 7 bars with 1.9 layer

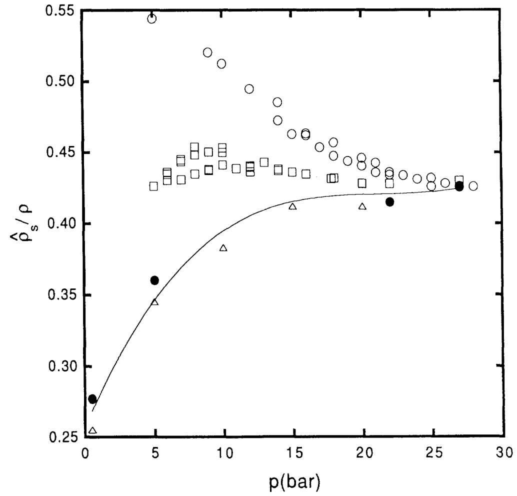

FIG. 3. Superfluid fraction as a function of pressure at T/T_c= 0.47 in 3 μm resonator. Closed circles (present work) and triangles (Ref. [10]) are data for pure ^{3}He and the line is a guide for the eye. Squares and open circles are for 1.9 and 2.6 layer ^{4}He coverage.

data, we do not observe significant hysteresis in contrast to the results of Tholen and Parpia [5]. Care was taken to wait (of order 1 d) for the internal equilibrium to establish after each change of pressure during which the temperature increased only to 3 mK.

The general pressure dependence in the silver cell is similar to the 3 μm cell aside from the small difference in overall magnitude of enhancement. The pressure at which enhancement disappears for a given ^{4}He coverage is almost the same in two powders. In 1 and 0.3 μm cells, there are substantial differences from the other two. With 1.9 layer ^{4}He coverage, the enhancement of the superfluid fraction is relatively small and it disappears at 12($\pm$ 2) bars in the 1 μm cell, and there is no enhancement from the pure ^{3}He data at any temperature or pressure in the 0.3 μm resonator. With 2.6 layer ^{4}He coverage the superfluid fraction enhancement is greater, but it disappears at 22 and 20 bars in 1 and 0.3 μm cells, respectively.

Our experiment allows us to extract the specularity from the Q measurement and relate the observed enhancement of the superfluid fraction to changes in the specularity factor in the same pore-surface structure. To compare with the slip theory, a combination of measured quantities, $(1/Q)(\hat{\rho}_s/\rho)/\omega(\rho_n/\rho)^2$, is plotted as circles in the inset to Fig. 4 as a function of reduced temperature for the 3 μm cell with pure ^{3}He at $p=$ 5 bars. According to the slip theory this quantity is equal to $\kappa\zeta R/8\eta$ and is shown by a solid line assuming $S = 0$. The pore radius was taken as 0.42 μm (as determined by mercury intrusion porosimetry) and there is no adjustable parameter. The data come quite close to the theory. A better fit (dashed line) is obtained if the pore radius is taken as 0.67 μm. The deviation at lowest temperatures might be an indication of inadequacy of the simple slip length formula used. The data at $p = 22$ bars give equally good agreement. The pore size dependence may be checked by plotting the same quantities at a given temperature and pressure in the 4 cells. The agreement in this case is within a factor of 2 over the pore size range. Given our resonator geometry, the frequency dependence is difficult to measure at a given temperature and pressure since the second and higher modes are increasingly affected by the thermal contact hole opening. The observed pressure dependence is consistent with the slip theory and provides an indirect measure of the frequency dependence (which arises from the first sound pressure dependence). With all the above supporting evidence it appears reasonable to extract S from the measured Q in the presence of ^{4}He coverage.

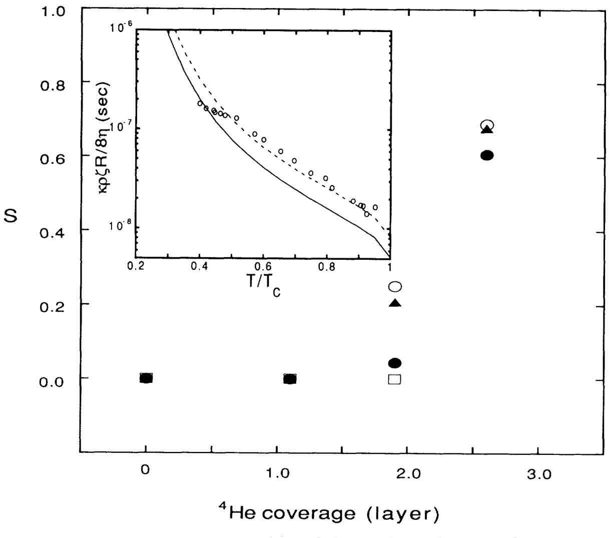

FIG. 4. Specularity deduced from fourth sound resonance quality factor. See text for inset.

We compute S from the measured quantities via

$$(1+S)/(1-S) = \{\hat{\rho}_s/Q\omega\rho_n^2\}_4/\{\hat{\rho}_s/Q\omega\rho_n^2\}_0, \qquad (2)$$

where 4 refers to ^{4}He coverage data and 0 to pure ^{3}He data. Note that we assumed that the slip length, the constant κ, and the pore radius R all remain the same with and without ^{4}He coverage and these quantities do not appear in Eq. (2). Our measurements show that as the ^{4}He coverage is increased Q decreases. The computed specularity is shown in Fig. 4 as a function of ^{4}He coverage for all cells at $T/T_c = 0.47$ and $p = 5$ bars. The points at 0 and 1.1 layer ^{4}He coverage all overlap. Q in the 0.3 μm cell at 2.6 layer coverage could not be determined owing to a poor signal level. We prove experimentally for the first time that the threshold thickness for the specularity to increase coincides with the superfluid fraction enhancement. The results are general and are not limited to smooth surfaces such as Mylar [2] and polished silicon [14].

It can be seen in Fig. 4 that S extrapolates to unity at about 3.2 layers in all but the 0.3 μm powder cell. The superfluid fraction in the specular limit is less than the bulk value in all powders and there exist remnant size effects. This result is contrary to the expectation [12] that depression of order parameter should be absent in the specular limit. A theoretical work on the remnant size effect in the specular limit would be interesting and our results should serve as a guide for the magnitude of effect as a function of pore size.

The pressure dependence of specularity reveals another interesting aspect of ^{4}He experiments. S, evaluated in the same manner as in the previous paragraph, is shown as a function of pressure in Fig. 5 for 2.6 layer ^{4}He coverage and the reduced temperature $T/T_c = 0.47$ in the 3 μm powder cell. As the pressure is changed the deduced specularity approaches linearly towards the pure ^{3}He value at about 25 bars. This pressure is very close to that at which the measured superfluid fraction reverts to the pure ^{3}He value. If superfluidity in the ^{4}He layer is what makes the surface more specular, then S should

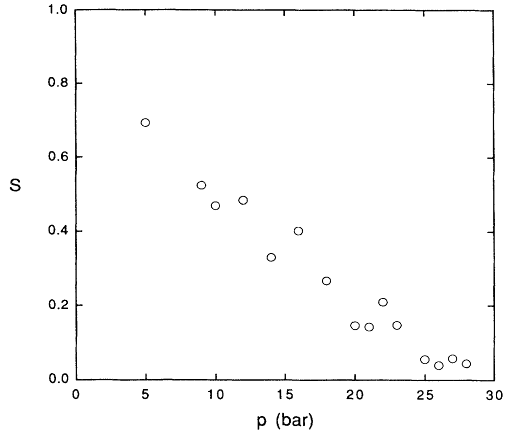

FIG. 5. Specularity as deduced from the same measurement as in Fig. 3 for 2.6 layer ^{4}He coverage. Only the data of decreasing pressure are shown for clarity.

sharply drop to zero over a narrow pressure range when the superfluid fraction in the ^{4}He layer vanishes at the freezing pressure of the ^{4}He layer. We do not observe such behavior. We speculate that superfluidity in the ^{4}He layer is gradually destroyed at higher pressures by greater penetration of ^{3}He into the ^{4}He layer. The solubility of ^{3}He in bulk ^{4}He does not change greatly as the pressure is increased, but we suspect that the "solubility" is much different in thin ^{4}He layers and moreover has a large pressure dependence.

In conclusion, we carried out the first simultaneous measurement of the enhancement of the superfluid fraction and the specularity factor of superfluid ^{3}He as a function of ^{4}He coverage. We show that below a pore size dependent threshold ^{4}He coverage there is no enhancement of the superfluid fraction. Once the threshold thickness is exceeded, both the measured specularity and superfluid fraction increase. As the specularity approaches unity, the superfluid fraction does not recover the bulk value and there is a pore size dependent remnant size effect. The enhancement in the ^{3}He superfluid fraction may be destroyed by increasing the ^{3}He pressure near to the bulk solidification pressure of ^{4}He. Surprisingly, the measured specularity smoothly approaches zero at the solidification pressure. As pointed out by Tholen and Parpia, pressurization of ^{4}He film with ^{3}He opens up a new approach to studies of thin boson systems.

One of us (H.K.) is supported in part by NSF Low Temperature Physics Program Grant No. DMR9204049. He is grateful to Peter Wölfle and Yuichi Okuda for very useful discussions and to Kedrick Brown for help in the analysis.

[1] V. Ambegaokar, P.G. de Gennes, and D. Rainer, Phys. Rev. A **9**, 2676 (1974).
[2] M.R. Freeman, R.S. Germain, E.V. Thuneberg, and R.C. Richardson, Phys. Rev. Lett. **60**, 596 (1988).
[3] D. Kim *et al.*, Physica (Amsterdam) **165&166B**, 637 (1990).
[4] S.C. Steel *et al.*, Physica (Amsterdam) **165&166B**, 599 (1990).
[5] S.M. Tholen and J. Parpia, Phys. Rev. Lett. **68**, 2810 (1992).
[6] Q. Jiang and H. Kojima, Phys. Rev. B **45**, 12616 (1992).
[7] T. Chainer, Y. Morii, and H. Kojima, J. Low Temp. Phys. **55**, 353 (1984).
[8] The index of refraction, a measure of tortuosity of the porous medium, is determined for each resonator in separate experiments with superfluid ^{4}He. Since the pore sizes are much smaller than the coherence length of ^{4}He, there are no appreciable size effects.
[9] H.H. Jensen, H. Smith, and P. Wölfle, J. Low Temp. Phys. **51**, 81 (1983).
[10] K. Ichikawa, S. Yamasaki, H. Akimoto, T. Kodama, T. Shigi, and H. Kojima, Phys. Rev. Lett. **58**, 1949 (1987).
[11] Vacuum Metallurgical Co. Ltd., Chiba 289-12, Japan. Sintering procedure increases the silver grain size (probably to about 0.2 μm).
[12] L.H. Kjäldman, J. Kurkijärvi, and D. Rainer, J. Low Temp. Phys. **33**, 577 (1978). Their theory gives $1.5\xi_0$ as the critical radius in the cylindrical pore with purely diffusive wall.
[13] ^{4}He was introduced into the cell as follows: (1) warm the cryostat to about 10 K, (2) pump out helium, (3) introduce an appropriate amount of ^{4}He into the cell, (4) cool the cell below 1 K , and (5) fill and pressurize the cell with ^{3}He. We followed Ref. [14] in converting from molar to layer coverage.
[14] S.M. Tholen and J. Parpia, Phys. Rev. Lett. **67**, 334 (1991).